Effects of collision on the time-independent states of a non-neutral plasma diode

Sourav Pramanik, Victor I. Kuznetsov, and Nikhil Chakrabarti

Citation: Physics of Plasmas **25**, 083512 (2018); doi: 10.1063/1.5038614
View online: https://doi.org/10.1063/1.5038614
View Table of Contents: http://aip.scitation.org/toc/php/25/8
Published by the American Institute of Physics

Effects of collision on the time-independent states of a non-neutral plasma diode

Sourav Pramanik,[1] Victor I. Kuznetsov,[2] and Nikhil Chakrabarti[3]
[1]*Department of Applied Mathematics, University of Calcutta, 92-Acharya Prafulla Chandra Road, Kolkata 700 009, India*
[2]*Ioffe Institute, 194021 St. Petersburg, Russia*
[3]*Saha Institute of Nuclear Physics, 1/AF Bidhannagar, Kolkata 700 064, India*

(Received 4 May 2018; accepted 30 July 2018; published online 14 August 2018)

A theoretical investigation is presented on the steady states of a planar plasma diode where static ions uniformly occupy the inter-electrode region. A cold and purely monochromatic electron beam is injected from the emitter plate, and the emitted electrons are carried to the collector plate through the uniform background of stationary ions. It is considered that the electrons suffer collisions with the other particles (with ions or neutral atoms) during its transportation through the inter-electrode gap. The effects of collisions are incorporated through a simplified one-dimensional model. With the help of Lagrangian description of fluid-Maxwell's equations, time-independent states are explored for arbitrary values of the neutralization parameter. Using the emitter electric field as a characteristic parameter, the steady-state solutions are categorized into "Bursian" and "Non-Bursian" branches in "emitter electric field vs diode gap" parametric space. The Non-Bursian solutions are found to be very sensitive to the dissipative term as they only exist for small, non-zero values of the normalized collision-frequency. *Published by AIP Publishing.* https://doi.org/10.1063/1.5038614

I. INTRODUCTION

In modern technology, there are so many sophisticated devices, such as Q-machines,[1–3] microwave generators,[4] electronic switches,[5] and particularly Thermionic Energy Converters (TIC)[6] where space charge limited (SCL) current plays an important role to control their operational conditions. In the field of space-research, the new generation of TIC efficiently fulfills the requirement of powerful sources which can produce electrical power of the order of 100 kW to 10 MW within the realistic size. TIC converts heat energy into electricity. When a cathode is heated to a high temperature (>1800 K), it emits energetic electrons. The emitted electrons are carried through a small electrode gap to be collected by a cooler anode surface. Generally, a TIC operates in a collisionless (Knudsen) regime with surface ionization. Theoretical analysis[6] suggests that with an emitter temperature of 2600 K, the TIC can achieve the specific power as high as 50 W/cm^2 and the efficiency close to ∼30%, when the collector temperature is kept around 1500 K. In practice, a binary Cs-Ba filling is used to achieve this limit.

In a realistic scenario, dissipative sources such as collision are inevitable, and this kind of dissipative sources can strongly influence the space charge limited flow, modifying the optimum operational conditions of plasma diode based instruments. In TIC, cesium atoms are used to create ions which neutralize the negative space charge of electrons near the emitter, and in this way, a strong increase in the electron current is ensured. The maximum specific power of the converter is achieved at the cesium pressure which corresponds to the transition regime between the collisionless (Knudsen) and the collisional states.[7] Therefore, it is necessary to study the influences of electron collisions on the operating mode of the TIC.

Besides, strong nonlinear oscillations of the electron current are observed in the Knudsen regime of the TIC.[8,9] The Bursian-Pierce instability plays a dominant role for the existence of these oscillations.[10–12] This instability is particularly developed in the plasma diode when the electrons are emitted with a very small velocity spread. If the velocity distribution function of the emitted electrons differs strikingly from the beam-like one, the instability cannot develop. The nonlinear oscillations in the Knudsen TIC are quenched when the electron scattering is reasonably strong or there is a magnetic field which is transverse to the electron trajectories.[8,9] Earlier, Ioffe Institute proposed an application where TIC can be used for alternate current generation (see, e.g., Ref. 13). The related mechanism is based on the development of diode instability for which electron current is cutoff for some specific values of relevant parameters. However, the operation of this proposed AC-current generator was considered in the Knudsen regime when the electrons flow through the diode with a small velocity spread. But in a realistic situation, it is very important to take into account the effects of the two crucial factors (transverse magnetic field and electron-scattering) on the excitation of instability in plasma diodes. Previously, we had studied the effect of the transverse magnetic field on the plasma diode states and their stability features.[14–17] It was shown in Ref. 18 that the physical dynamics of a TIC can be successfully modeled by means of the Pierce-like diode in which injected electrons have the beam-like velocity distribution. Here, in our analytic investigation, we replicate a TIC by a planar model of the Pierce-like plasma diode and investigate the effects of the electron collision on the steady-state characteristics.

Pierce diode is a non-neutral plasma diode where a beam of monoenergetic electrons is transported through the background

of uniformly distributed immobile ions. It was Pierce who studied such kind of system first theoretically[12] and found that a limiting value of the steady-state current exists beyond which current density falls substantially due to the generation of an aperiodic instability (Pierce Instability).[12,19,20] The term "Pierce" was first introduced by Kuhn[21] for this kind of diodes. The stationary states of Pierce diode (collisionless) is generally represented through the "emitter field strength vs diode gap" diagram.[22] It is observed that they can be divided into two major parts: Bursian and non-Bursian family of solutions. The general features of Bursian family are similar to the solutions of Bursian diodes. The non-Bursian solutions in the Pierce diode arise because of wavy potential distributions (PDs).[22,23]

For a given applied voltage between the electrodes, the Bursian curves in "emitter field strength-diode gap" parametric plane contain two bifurcation points. The right bifurcation points are called *SCL*-point (space charge limit), and it signifies the state with the maximum diode current. Each curve ends at "zero-point" (for purely monoenergetic beam), and it corresponds to the situation when the longitudinal electron velocity vanishes due to the formation of a strong potential barrier (virtual cathode). Beyond this point, there is no steady state as all the electrons are reflected back to the emitter end.[24,25]

As the electrons are injected by the emitter, they travel through the inter-electrode gap to reach the collector. On their path, they may suffer collisions with ions and other neutral atoms. Previously, an analytical theory for the space charge limited flow in a vacuum diode (Bursian diode)[11] was developed by Akimov and Schamel to incorporate the effects of collision.[26] They presented the improved *SCL* characteristics by using one-dimensional cold fluid equations where the collisional effect was treated by a rather simple model (Drudes model). The effect of collision was modeled by a friction parameter ν, which was assumed to be constant. Although such a one-dimensional model is rather a simplified approximation to describe the actual process of electron scattering, utilizing this model we can check qualitatively how collision alters the time-independent states of the plasma diode. We have to keep in mind that such a model is valid more or less for the case when the collisional frequency is less than the electron beam frequency or it is of the order of the electron beam frequency. In this present work, we employ a similar kind of analytical approach to study the time-independent solutions of a generalized Pierce diode[22] in the presence of collisional effects. A comprehensive analysis reveals that the presence of collisional drag can cause the disappearance of the non-Bursian branches.

The article is organized as follows: Section II presents the electron dynamics in the presence of the self-consistent electric field. In Sec. III, the analytical solutions are derived for the steady states with the help of Lagrangian description and their properties are investigated. In Sec. IV, the results obtained are briefly summarized.

II. TREATMENT OF THE PROBLEM AND DIMENSIONLESS VARIABLES

We assume that two infinite planar electrodes are placed at a distance d from each other. A potential difference U is applied across them. The z-axis is perpendicular to the emitter surface ($z=0$). A non-relativistic and mono-energetic electron beam enters from the emitter with the density n_b and injection velocity v_b perpendicularly to the emitter surface. They are collected either at the collector or at the emitter when they are turned around by the virtual cathode. The electric field E can be calculated from the scalar potential φ which depends on the z coordinate only.

We also assume that the diode region is uniformly occupied by the infinitely massive ions of constant density n_i. The ions are assumed to be immobile. A practical situation where ions do not participate in the diode dynamics can be created when ions are injected perpendicularly to the direction of electron emission.[22] If their velocities are large enough, they will leave the diode region without any considerable change in their density distribution providing a homogeneous ion distribution in the background. The ion background is taken into account through the dimensionless neutralization parameter

$$\gamma = n_i/n_b. \tag{1}$$

We should note that γ can take any arbitrary physical value and the situation of charge neutralization ($\gamma = 1$) is merely a situation among many possible options. We refer such a device as the Pierce diode,[12] whereas, for the Bursian diode, the neutralization factor γ is zero (i.e., ions are totally absent).[11]

In 1D, the time-independent states of a collisionless Pierce diode are governed by the continuity, momentum, and the Poisson's equations

$$\frac{d}{dz}(nv_z) = 0, \quad v_z\frac{dv_z}{dz} = -\frac{e}{m}E, \quad E = -\frac{d\varphi}{dz},$$
$$\frac{dE}{dz} = -\frac{e}{\epsilon_0}(n - \gamma n_b). \tag{2}$$

To express all relevant variables in terms of dimensionless quantities, we introduce energy and length units which are the kinetic energy of electrons at the emitter W_b and the beam Debye length λ_D, respectively,[24,27]

$$\lambda_D = \left[\frac{2\epsilon_0 W_b}{e^2 n_b}\right]^{1/2} \approx 0.3238 \times 10^{-2}\frac{V_b^{3/4}}{j_b^{1/2}}[\text{cm}],$$
$$W_b = mv_b^2/2. \tag{3}$$

Here, the current density $j_b = en_bv_b$ and accelerating voltage $V_b = W_b/e = mv_b^2/(2e)$ of the injected beam are taken in Amperes per square cm and Volts, respectively; the symbols e and m represent the electron charge and electron mass; the free-space permittivity $\epsilon_0 = 8.854 \times 10^{-12}\text{C}^2/\text{Nm}^2$.

The dimensionless coordinate, time, velocity, potential, and electric field strength are introduced as $\zeta = z/\lambda_D$, $t = t\omega_b$, $u = v_z/\sqrt{2W_b/m}$, $\eta = e\varphi/(2W_b)$, $\varepsilon = eE\lambda_D/(2W_b)$, where $\omega_b = [e^2n_b/(m\epsilon_0)]^{1/2}$ is the characteristic frequency. The dimensionless inter-electrode gap and voltage between the collector and emitter are denoted via δ and V, respectively.

In the steady-state condition, the presence of collisions can be incorporated in the momentum equation by a dissipative term which is proportional to the electron velocity.[26]

Therefore, our basic governing equations can be expressed in dimensionless form as

$$\frac{d}{d\zeta}(nu)=0,\quad u\frac{du}{d\zeta}=-\varepsilon-\nu u,\quad \varepsilon=-\frac{d\eta}{d\zeta},\quad \frac{d\varepsilon}{d\zeta}=-n+\gamma. \tag{4}$$

The coefficient ν is defined as $\nu=\langle\nu\rangle/\omega_b$, where $\langle\nu\rangle$ denotes the average "collisional frequency," and it is defined as $\langle\nu\rangle=\langle v\rangle/\langle\lambda\rangle$. Note that it has the dimension of "Time^{-1}." Here, the parameter $\langle\lambda\rangle$ is the mean free path of electrons, and $\langle v\rangle$ characterizes the velocity spread due to collision process. For our model, we can write $\langle v\rangle=u_b\langle\lambda\rangle/\lambda_D\sim u_b/(\lambda_D\sigma n_b)$, with σ being the collision scattering cross section.

To be realistic, we can treat a plasma diode collisionless as long as the characteristic Debye length (λ_D) is much less than the average mean free path of the electrons, i.e., $\lambda_D\ll\bar{\lambda}$ (say, $\bar{\lambda}=\langle\lambda\rangle$). Equivalently, we can say that for a collisionless plasma diode, beam characteristic frequency (ω_b) is larger than the collisional frequency ($\langle\nu\rangle$), i.e., $\omega_b\gg\langle\nu\rangle$. The effect of collision starts to dominate the picture when $\omega_b\sim\langle\nu\rangle$. For analytical purpose, it is safe to assume ν to be constant as long as $\nu\le 1$.[26] The boundary conditions at the emitter to be used are density $n(\zeta=0)=1$, velocity $u(\zeta=0)=1$, electric potential $\eta(\zeta=0)=0$, and electric field $\varepsilon(\zeta=0)=\varepsilon_0$. The emitter electric field ε_0 will be used as a variable parameter for our following analysis. The boundary condition at the collector is $\eta(\zeta=\delta)=V$.

We should note that in the absence of collision ($\nu=0$), the second and third equations of Eq. (4) yield the energy conservation

$$\frac{1}{2}u^2-\eta=\frac{1}{2}. \tag{5}$$

In the absence of collision, it follows from this equation that the PDs $\eta(\zeta)$ should be confined within a region limited by a straight line $p(\zeta;\Omega)$

$$\eta(\zeta)\ge p(\zeta;\gamma)\equiv\eta_c, \tag{6}$$

where $\eta_c=-1/2$ for conservative case. Interestingly, this condition does not depend on the ion background. But in the presence of dissipative source like collision, the conservation of energy does not hold and the value of η_c differs from the conservative case.

III. FEATURES OF STEADY STATE: LAGRANGIAN DESCRIPTION

To solve the non-linear equations (5), we introduce the Lagrangian coordinate τ and the Lagrange transformation

$$\zeta=\int_0^\tau u(\tau')d\tau'.$$

Thus, $ud/d\zeta=d/d\tau$. Then, Eq. (5) takes the form

$$\frac{d}{d\tau}(nu)=0,\quad \frac{du}{d\tau}=-\varepsilon-\nu u,\quad \frac{d\eta}{d\tau}=-u\varepsilon,\quad \frac{d\varepsilon}{d\tau}=-1+\gamma u. \tag{7}$$

Combining Eq. (7), we can have

$$\frac{d^2u}{d\tau^2}+\nu\frac{du}{d\tau}+\gamma u=1. \tag{8}$$

The relevant initial conditions are

$$u(0)=1,\quad \frac{d}{d\tau}u(0)=-\varepsilon_0-\nu. \tag{9}$$

Using these initial conditions, we integrate Eq. (8) and find the velocity u in terms of the Lagrangian coordinate. Then, integrating it we can calculate the position of an electron. For $\nu<2\sqrt{\gamma}$, we obtain

$$\begin{aligned}u(\tau)=&\frac{1}{\gamma}-\frac{1}{\gamma}\left\{(1-\gamma)\cos(\beta\tau)+\frac{1}{\beta}\left[(\gamma\varepsilon_0+\nu)-\frac{\nu}{2}(1-\gamma)\right]\right.\\&\left.\times\sin(\beta\tau)\right\}\exp\left(-\frac{\nu}{2}\tau\right),\\ \zeta(\tau)=&\frac{1}{\gamma}\tau-\frac{1}{\gamma^2}(\gamma\varepsilon_0+\nu)+\frac{1}{\gamma^2}\exp\left(-\frac{\nu}{2}\tau\right)\\&\times\left\{(\gamma\varepsilon_0+\nu)\cos(\beta\tau)+\frac{1}{\beta}\left[\frac{\nu}{2}(\gamma\varepsilon_0+\nu)-\gamma(1-\gamma)\right]\right.\\&\left.\times\sin(\beta\tau)\right\}.\end{aligned} \tag{10}$$

On the other hand, for $\nu>2\sqrt{\gamma}$, the functions $u(\tau)$ and $\zeta(\tau)$ read

$$\begin{aligned}u(\tau)=&\frac{1}{\gamma}+\frac{1}{\alpha\gamma}\left[(\gamma\varepsilon_0+\nu)-\frac{1}{2}(1-\gamma)(\nu+\alpha)\right]\exp\left(-\frac{\nu+\alpha}{2}\tau\right)\\&-\frac{1}{\alpha\gamma}\left[(\gamma\varepsilon_0+\nu)-\frac{1}{2}(1-\gamma)(\nu-\alpha)\right]\exp\left(-\frac{\nu-\alpha}{2}\tau\right),\\ \zeta(\tau)=&\frac{1}{\gamma}\tau-\frac{1}{\gamma^2}(\gamma\varepsilon_0+\nu)-\frac{1}{\alpha\gamma^2}\left[\frac{1}{2}(\nu-\alpha)(\gamma\varepsilon_0+\nu)-\gamma(1-\gamma)\right]\\&\times\exp\left(-\frac{\nu+\alpha}{2}\tau\right)+\frac{1}{\alpha\gamma^2}\left[\frac{1}{2}(\nu+\alpha)(\gamma\varepsilon_0+\nu)-\gamma(1-\gamma)\right]\\&\times\exp\left(-\frac{\nu-\alpha}{2}\tau\right).\end{aligned} \tag{11}$$

Here, we introduce two parameters which are effective "frequency" β and α

$$\beta=\sqrt{\gamma-\nu^2/4},\quad \alpha=\sqrt{\nu^2-4\gamma}. \tag{12}$$

Now the fourth equation of Eq. (7) gives the electric field in terms of the Lagrangian variable: $\varepsilon(\tau)=\varepsilon_0-\tau+\gamma\zeta(\tau)$. At last, from the relation $d\eta/d\tau=-u\varepsilon$, we obtain for the potential

$$\begin{aligned}\eta(\tau)&=-\varepsilon_0\zeta(\tau)-\frac{1}{2}\gamma\zeta^2(\tau)+\int_0^\tau tu(t)dt\\&=-\frac{1}{2}\gamma\zeta^2(\tau)+(\tau-\varepsilon_0)\zeta(\tau)-\int_0^\tau\zeta(t)dt.\end{aligned} \tag{13}$$

At the collector position [$\tau=T$, $\zeta(T)=\delta$, $\eta(\delta)=V$], we have

$$V=-\frac{1}{2}\gamma\delta^2+(T-\varepsilon_0)\delta-\int_0^T\zeta(t,\varepsilon_0)dt,\quad \delta=\zeta(T,\varepsilon_0). \tag{14}$$

Here, T is the time-of-flight of an electron between the electrodes and the function $\zeta(\tau)$ is determined from Eq. (10) or (11). Note that in the limit $\nu \to 0$, the formula (10) coincide totally with Eq. (41) in Ref. 22.

Using Eqs. (10)–(13), we can calculate the electron velocity, the density profile, the electric field, and the potential within the inter-electrode space. For particular values of γ, ν, and ε_0, we can determine the profiles of relevant quantities by gradually increasing τ up to the moment ($\tau = T$) when the potential η [Eq. (13)] takes the value equal to the collector potential V. As a result, we find the value of the inter-electrode gap δ, as well as the time T when an electron arrives at the collector surface.

Figure 1 demonstrates the corresponding profiles of the potential $\eta(\zeta)$ [Figs. 1(a) and 1(b)] and the velocity $u(\zeta)$ [Figs. 1(c) and 1(d)] of the electrons within the inter-electrode region for both positive and negative values of ε_0 with $\gamma = 1.1$. The potential profile shows a wavy nature for $\nu = 0$ and relatively small values of ν. With increasing ν, the wavy nature of the potential profile is gradually lost. From the velocity profile, it is observed that, for a fixed value of γ, the velocity curves contain several minima. However, for some particular values of the ν, the minimum value of the velocity reaches to zero. The state corresponding to this situation is called "zero-point." In Figs. 1(e) and 1(f), the velocity and potential plots are shown for a zero-point state. The "zero-point" state appears when the kinetic energy of the emitted electron becomes zero at some position within the inter-electrode region.

The formation of potential minima within the diode region acts as a potential barrier to the emitted electrons. As long as the kinetic energy of the emitted electrons is greater than the height of the potential minima, electrons can cross the potential barrier and reach the collector end. Suppose the

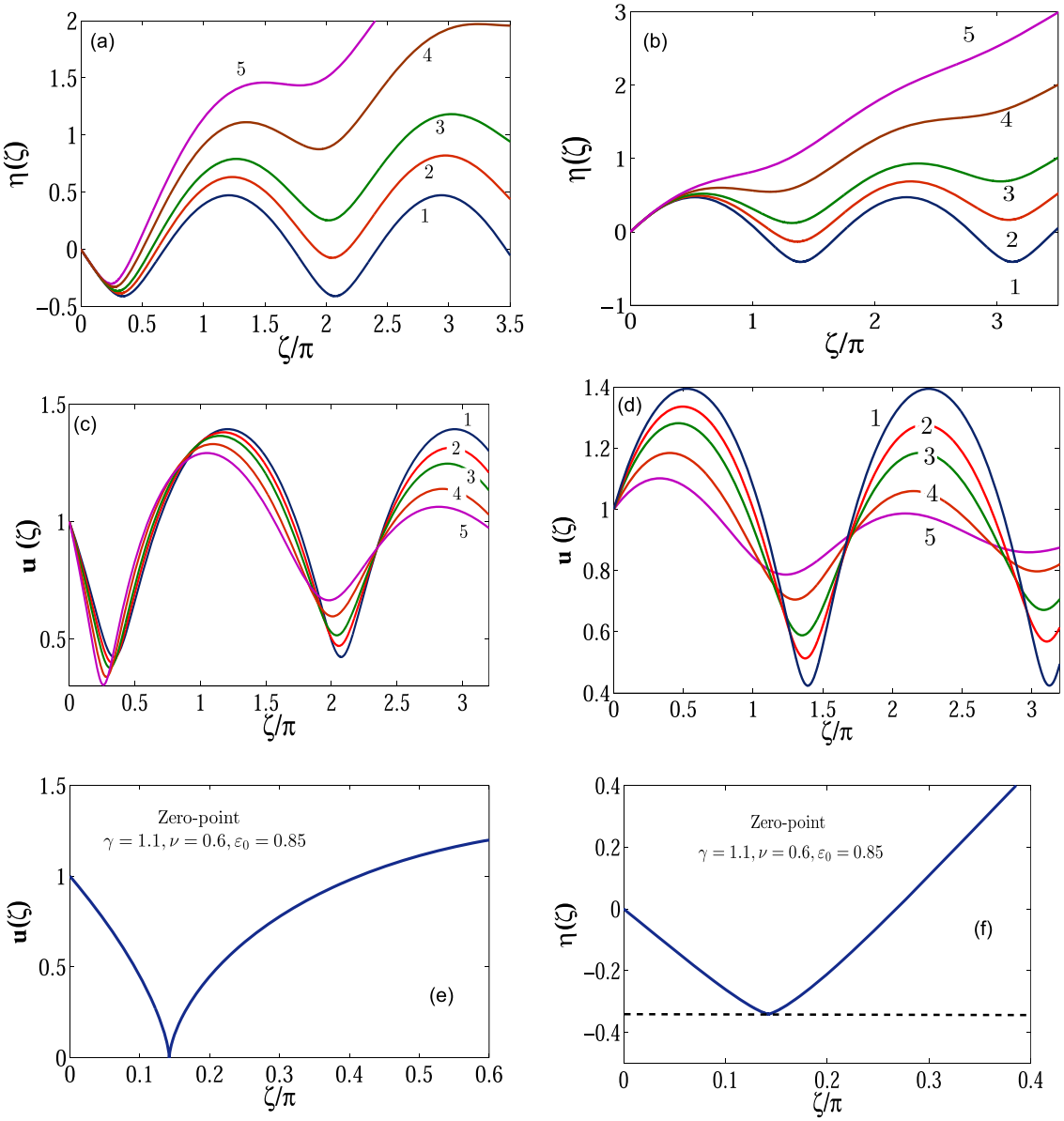

FIG. 1. (a) and (b) display potential distribution and (c) and (d) display electron velocity profile within the inter-electrode space drawn for $\gamma = 1.1$ and various values of ν: (1) $\nu = 0$, (2) 0.05, (3) 0.1, (4) 0.2, (5) 0.3. (a) and (c): $\varepsilon_0 = 0.5$, (b) and (d): $\varepsilon_0 = -0.5$. (e) and (f) respectively show the velocity and potential distribution for a "zero-point" state: $\gamma = 1.1$, $\varepsilon_0 = 0.85$ and $\nu = 0.6$. Dashed line in (f) corresponds to $\eta = \eta_c = -0.34$.

kinetic energy of the emitted electrons is completely exhausted and electron velocity vanishes, when the minimum value of the potential reaches a critical value η_c at some point. In this condition, the potential barrier is now strong enough to block the electron flow. In the absence of collision, $\eta_c = -1/2$, i.e., the height of the potential barrier becomes equal to the kinetic energy of the injected beam [see Eq. (6)] and the velocity of the electron becomes zero at the position of the virtual cathode (potential minimum). However, in the presence of collision, the system is non-conservative. The emitted electrons suffer a dragging effect due to collision with the ions and other neutral atoms as they move towards the collector. As a result, the kinetic energy is dissipated along their paths. Evidently, for the collisional effect, "zero-point" state occurs at a lower value of the potential barrier than the conservative one (i.e., $|\eta_c| < 0.5$). If the emitted electron beam is purely monoenergetic, i.e., all electrons are emitted with the same velocity, all of them are reflected back to the emitter when the minimum value of the potential reaches the value η_c. To the right of the position of the zero velocity, there are no electrons. So, the electron density to the right of this point is zero and hence the diode current becomes zero. Beyond this limit, no steady state exists, and thus zero-point serves as the boundary of our analysis. However, if there is a small spread in the velocity distribution function of the emitted electron beam, a small portion of the emitted electrons (with the velocity little higher than v_b) can overcome the potential barrier and reach the collector producing very small amount of current. This is the case of partial electron reflection which arises because of the non-monochromatic nature of the emitted electron beam. Figures 2(a) and 2(b) display the velocity and potential plots corresponding to a number of "zero-point" states for $\gamma = 1.1$.

Let us consider the zero velocity occurs at the point $\zeta = \zeta_0$ for emitter electric field strength $\varepsilon_0 = \varepsilon_{0,0}$, and the corresponding value of τ is τ_0, i.e., $\zeta(\tau = \tau_0) = \zeta_0$. The condition for "zero-point" states can be obtained from the following relations: $u(\tau = \tau_0) = 0$ and $du/d\tau(\tau = \tau_0) = 0$. For the case $\nu < 2\sqrt{\gamma}$, these two conditions give us the following relations:

$$(1-\gamma)\cos(\beta\tau_0) + \frac{1}{\beta}\left[(\gamma\varepsilon_0+\nu) - \frac{\nu}{2}(1-\gamma)\right]\sin(\beta\tau_0) = \exp\left(\frac{\nu}{2}\tau_0\right),$$
$$(\varepsilon_0+\nu)\cos(\beta\tau_0) - \frac{1}{\beta}\left[\frac{\nu}{2}(\varepsilon_0+\nu)+1-\gamma\right]\sin(\beta\tau_0) = 0. \tag{15}$$

Equation (15) provides

$$\cos(\beta\tau_0) = \frac{\frac{\nu}{2}(\varepsilon_0+\nu)+1-\gamma}{D}\exp\left(\frac{\nu}{2}\tau_0\right),$$
$$\sin(\beta\tau_0) = \frac{\beta(\varepsilon_0+\nu)}{D}\exp\left(\frac{\nu}{2}\tau_0\right),$$
$$D = (\varepsilon_0+\nu)(\gamma\varepsilon_0+\nu) + (1-\gamma)^2 > 0. \tag{16}$$

Equation (16) allows us to find τ_0 as a function on ε_0. Depending on the values of γ, the function $\tau_0(\gamma,\nu)$ takes the form for $\varepsilon_0 > -\nu$

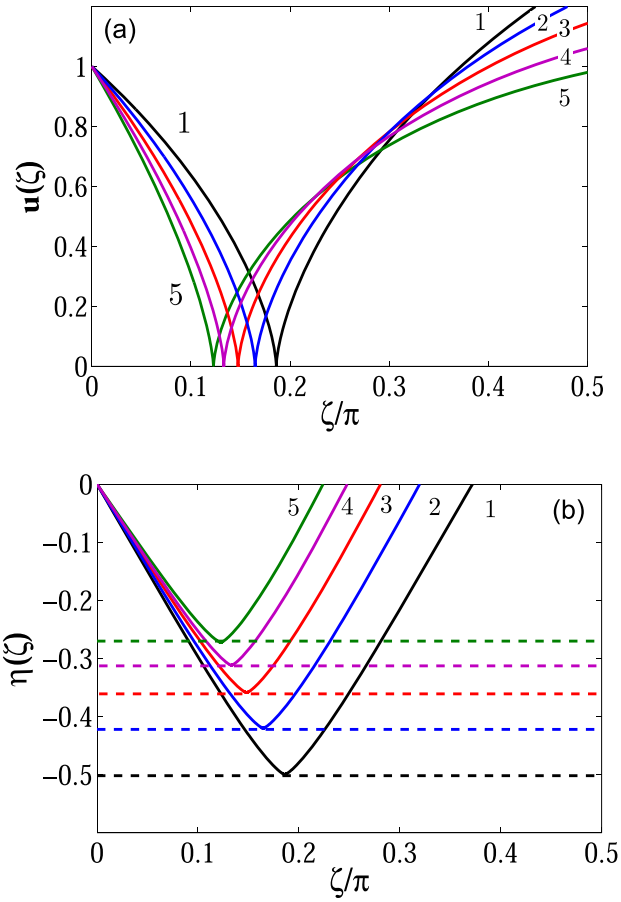

FIG. 2. Velocity profile (a) and potential profile (b) for the situation when electron velocity vanishes for the first time (zero-point). Dashed lines in (b) correspond to relevant values of η_c. Curves: $1(\nu = 0, \varepsilon_0 = 0.95; \eta_c = -0.5)$, $2(\nu = 0.25, \varepsilon_0 = 0.904; \eta_c = -0.42)$, $3(\nu = 0.5, \varepsilon_0 = 0.864; \eta_c = -0.36)$, $4(\nu = 0.75, \varepsilon_0 = 0.83; \eta_c = -0.31)$, $5(\nu = 1, \varepsilon_0 = 0.796; \eta_c = -0.273)$; $\gamma = 1.1$.

$$\beta^{-1}\arctan\left\{\beta(\varepsilon_0+\nu)\Big/\left[\frac{\nu}{2}(\varepsilon_0+\nu)+1-\gamma\right]\right\},$$
$$\text{if } \gamma < 1+(\nu/2)(\varepsilon_0+\nu),$$
$$\beta^{-1}\left(\pi - \arctan\left\{\beta(\varepsilon_0+\nu)\Big/\left|\frac{\nu}{2}(\varepsilon_0+\nu)+1-\gamma\right|\right\}\right),$$
$$\text{if } \gamma > 1+(\nu/2)(\varepsilon_0+\nu). \tag{17}$$

On the other hand, for $\varepsilon_0 < -\nu$ the function $\tau_0(\gamma,\nu)$ becomes

$$\beta^{-1}\left(\pi + \arctan\left\{\beta|\varepsilon_0+\nu|\Big/\left|\frac{\nu}{2}(\varepsilon_0+\nu)+1-\gamma\right|\right\}\right),$$
$$\text{if } \gamma > 1+(\nu/2)(\varepsilon_0+\nu),$$
$$\beta^{-1}\left(2\pi - \arctan\left\{\beta|\varepsilon_0+\nu|\Big/\left[\frac{\nu}{2}(\varepsilon_0+\nu)+1-\gamma\right]\right\}\right),$$
$$\text{if } \gamma < 1+(\nu/2)(\varepsilon_0+\nu). \tag{18}$$

The value of $\varepsilon_{0,0}$ can be calculated by utilizing the 2nd equation of Eq. (15) where the corresponding form of $\tau_0(\gamma,\nu)$ is determined by Eq. (17) or (18).

For the case $\nu > 2\sqrt{\gamma}$, the conditions for zero-point states lead us to the following equations:

$$\left[(\gamma\varepsilon_0+\nu)-\frac{\nu+\alpha}{2}(1-\gamma)\right]\exp\left(-\frac{\nu+\alpha}{2}\tau_0\right) - \left[(\gamma\varepsilon_0+\nu)-\frac{\nu-\alpha}{2}(1-\gamma)\right]\exp\left(-\frac{\nu-\alpha}{2}\tau_0\right) = -\alpha,$$
$$\left[\frac{\nu+\alpha}{2}(\varepsilon_0+\nu)+1-\gamma\right]\exp\left(-\frac{\nu+\alpha}{2}\tau_0\right) - \left[\frac{\nu-\alpha}{2}(\varepsilon_0+\nu)+1-\gamma\right]\exp\left(-\frac{\nu-\alpha}{2}\tau_0\right) = 0. \quad (19)$$

We can obtain the following relations from Eq. (19):

$$\exp\left(-\frac{\nu+\alpha}{2}\tau_0\right) = \frac{(\nu-\alpha)(\varepsilon_0+\nu)/2+1-\gamma}{(\gamma\varepsilon_0+\nu)(\varepsilon_0+\nu)+(1-\gamma)^2},$$
$$\exp\left(-\frac{\nu-\alpha}{2}\tau_0\right) = \frac{(\nu+\alpha)(\varepsilon_0+\nu)/2+1-\gamma}{(\gamma\varepsilon_0+\nu)(\varepsilon_0+\nu)+(1-\gamma)^2}. \quad (20)$$

Whereas Eq. (20) can provide a relation between τ_0 and $\varepsilon_{0,0}$

$$\tau_0 = \frac{2}{\nu+\alpha}\ln\left\{\frac{(\gamma\varepsilon_{0,0}+\nu)(\varepsilon_{0,0}+\nu)+(1-\gamma)^2}{(\nu-\alpha)(\varepsilon_{0,0}+\nu)/2+1-\gamma}\right\}. \quad (21)$$

We can determine $\tau_0(\gamma,\nu)$ and $\varepsilon_{0,0}$ from Eq. (21) and the first equation of Eq. (19), respectively.

Solving Eqs. (15)–(18) or (19) and (20), we can find the values of τ_0 and $\varepsilon_{0,0}$ for fixed values of γ and ν. The variations of emitter electric field strength for zero-point states $(\varepsilon_{0,0})$, threshold value of potential minima (η_c), and the position of zero velocity ζ_0 are displayed with respect to the dimensionless collision frequency (ν) in Figs. 3(a), 3(b), and 3(c) for several γ values.

The time-independent states of Pierce-like diodes are generally visualized through the $\{\varepsilon_0,\delta\}-$ parametric curves.[23,24] For a purely monoenergetic electron beam, each of these curves ends at "zero-point" $(\varepsilon_{0,0},\delta_0)$. The stationary states in $\{\varepsilon_0,\delta\}-$ plane can also be distinguished into Bursian and non-Bursian parts. The Bursian curves are generally gathered around $0<\delta/\pi<1$. The right boundary of the Bursian curve represents the SCL-point or Space-Charge-Limit, where $d\delta/d\varepsilon_0 = 0$. It corresponds to the steady state where the plasma diode can sustain a maximum current density. By varying the values of V, we can generate several Bursian curves of similar general features. When the values of V are changed, the locations of SCL and zero-point of the curve also change.

In the Bursian diode, where the emitted electrons move towards the collector in the absence of positively charged ions in the background, only the Bursian family of solutions appears. The potential profile of the Bursian diode carries single minimum point within the inter-electrode region, and for this reason, only the Bursian family of solutions is observed.[11,14] But due to the presence of background ions, the potential profile of the Pierce diode is significantly different from the Bursian diode. The spatial potential profile of

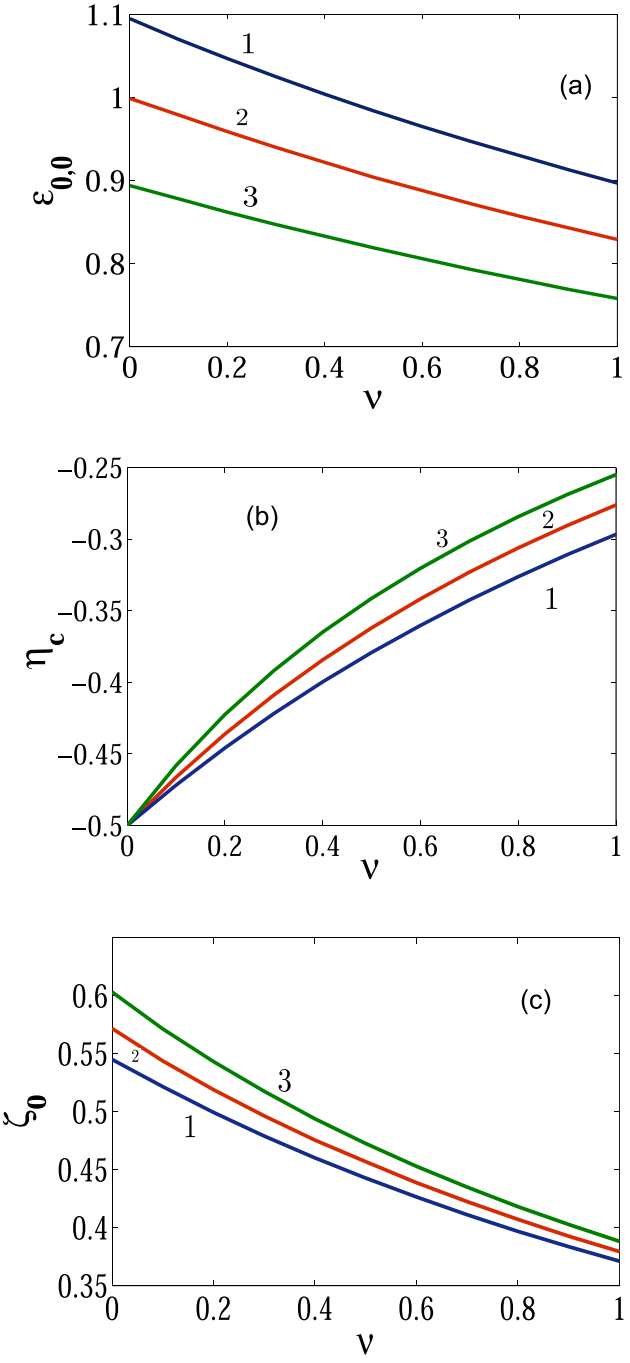

FIG. 3. (a) Emitter field strength at zero-points $(\varepsilon_{0,0})$ vs collision frequency (ν) for different $\gamma-$ values; curve: 1 ($\gamma = 0.8$), 2 ($\gamma = 1$), 3 ($\gamma = 1.2$). (b) η_c vs ν for different γ-values; curve: 1 ($\gamma = 0.2$), 2 ($\gamma = 1$), 3 ($\gamma = 1.6$). (c) Position of zero-velocity ζ_0 vs ν for different γ-values; curve: 1 ($\gamma = 0.8$), 2 ($\gamma = 1$), 3 ($\gamma = 1.2$).

the Pierce like diode exhibits wavy nature with several local minima and maxima, supporting more than one group of solutions for fixed V. The $\varepsilon_0-\delta$-parametric diagram shows that along with the family of solutions like Bursian ones (located around $0<\delta/\pi<1$), a group of solutions exists for other regions of δ (around $1<\delta/\pi<3.2$) also. Unlike the Bursian diode, steady state solutions also exist for negative values of ε_0 in the Pierce diode. This new family of solutions is called as the non-Bursian family.[16,22]

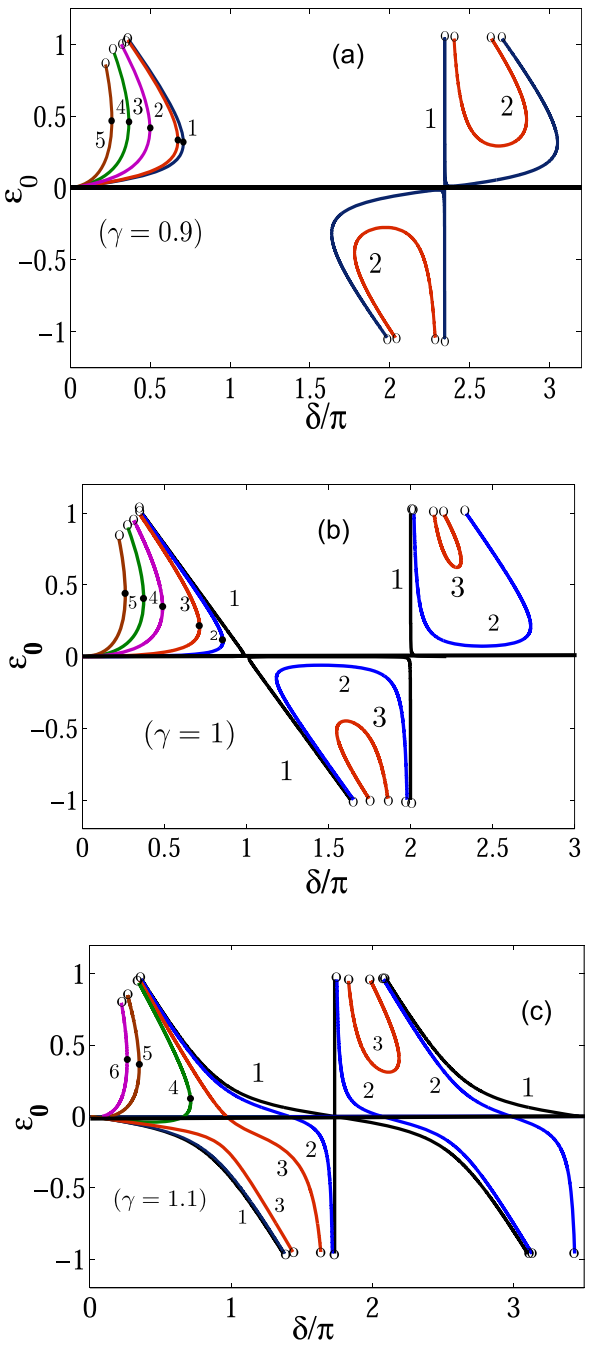

FIG. 4. Curves $\varepsilon_0(\delta)$ drawn for three values of γ and various values of ν: (a) $\gamma = 0.9$; $\nu = 0$ (curve 1), 0.04 (2), 0.2 (3), 0.5 (4), and 1 (5); (b) $\gamma = 1.0$; $\nu = 0$ (curve 1), 0.04 (2), 0.1 (3), 0.25 (4), 0.5 (5), and 1 (6); (c) $\gamma = 1.1$; $\nu = 0$ (curve 1), 0.01 (2) 0.05 (3), 0.1 (4), 0.6 (5), and 1 (6). Each curve ends at zero-point; $V = 0$. The SCL-points of Bursian curves are marked by solid circles and zero-points are marked by open circles.

In our case, the relevant parameters are γ, ν, and V. In Fig. 4, the steady-states are depicted through the "$\varepsilon_0 - \delta$"-continuous curves for three separate values of γ and a number of ν values taking applied external voltage $V = 0$. Here, each curve ends at "zero-point," i.e., at $\varepsilon_0 = \varepsilon_{0,0}$. Both the Bursian (located around $0 < \delta/\pi < 1$) and non-Bursian (located around $1 < \delta/\pi < 3.2$) branches of solutions are displayed in Fig. 4. The Bursian family contains a region of non-unique solutions between SCL-point (on the right boundary) and zero-point (on the left boundary), i.e., within $\varepsilon_{0,SCL} \le \varepsilon_0 \le \varepsilon_{0,0}$. As the value of ν is gradually increased, the locations of *SCL* and zero-point change in the $\varepsilon_0 - \delta$ parametric plane. One can see that non-Bursian states only exist when ν has rather small values ($\nu < 0.1$) and disappear for higher values of ν [$\nu = \langle\nu\rangle/\omega_b$]. The non-Bursian states appear in Pierce diode because of the wavy potential profile. We can see from Figs. 1(a) and 1(d) that the wavy nature of potential is gradually lost with the increase in ν.

It is interesting to compare these steady states [represented by $\varepsilon_0(\delta)$ curves in Fig. 4] with the states of the non-neutral Pierce-like diode in the presence of an external transverse magnetic field (see Fig. 3 in Ref. 16). In the latter case, the solutions are controlled by a parameter $\Omega = \omega_L/\omega_b$, where ω_L and ω_b are the Larmor frequency and beam characteristic frequency, respectively. One can see that the steady state solutions of these two cases resemble each other and exhibit similar kind of characteristics with respect to relevant controlling parameters (ν and Ω). The reason lies in the fact that both the external magnetic field and the electron-collision modify the beam-like velocity distribution function of the injected electron beam. However, two cases are not same. In the presence of collisions, the system is a non-conservative type and the energy of the emitted electron is continuously dissipated as it proceeds towards the collector, whereas the transverse magnetic field splits the electron energy along two mutually perpendicular directions in such a way that total energy is conserved.

Now we determine the coordinates of the *SCL* point. Looking at Fig. 4, we see that the condition $d\delta/d\varepsilon_0 = 0$ has to hold at this point. We can calculate this derivative from Eq. (14)

$$\frac{d\delta}{d\varepsilon_0} = \frac{\partial\delta}{\partial\varepsilon_0} + \frac{\partial\delta}{\partial T}\frac{dT}{d\varepsilon_0} = \frac{\partial\delta}{\partial\varepsilon_0} - \frac{\partial\delta}{\partial T}\frac{(\partial V/\partial\varepsilon_0)}{(\partial V/\partial T)} = 0. \tag{22}$$

Calculating the partial derivatives in Eq. (22), we have

$$\begin{aligned}\frac{\partial V}{\partial T} &= (T - \varepsilon_0 - \gamma\delta)\cdot u,\\ \frac{\partial V}{\partial\varepsilon_0} &= (T - \varepsilon_0 - \gamma\delta)\frac{\partial\delta}{\partial\varepsilon_0} - \delta - \int_0^T \frac{\partial}{\partial\varepsilon_0}\zeta(t)dt.\end{aligned} \tag{23}$$

Substituting these values in Eq. (22) and reducing the similar terms in the numerator, we obtain

$$\zeta(T,\varepsilon_0) + \frac{\partial}{\partial\varepsilon_0}\int_0^T \zeta(t,\varepsilon_0)dt = 0. \tag{24}$$

Equation (24) gives the relation between the emitter electric field strength ε_0 and the time-of-flight T. In order to find this relation, we need to utilize the formulae for $\zeta(\tau,\varepsilon_0)$ derived earlier. After simplifying the mathematical terms, we obtain from Eq. (10)

$$\varepsilon_0\cos(\beta T) + \frac{1}{\beta}\left(\frac{\nu}{2}\varepsilon_0 + \gamma\right)\sin(\beta T) = \varepsilon_0\exp\left(\frac{\nu}{2}T\right), \tag{25}$$

for $\nu < 2\sqrt{\gamma}$. Note that, in the limit $\nu \to 0$, the parameter $\beta \to \sqrt{\gamma}$ and Eq. (25) converges into Eq. (20) of Ref. 16 with

$\alpha = \sqrt{\gamma}$. Using the form of $\zeta(\tau, \varepsilon_0)$ from Eq. (11) and performing the same procedure for $\nu > 2\sqrt{\gamma}$, we obtain from Eq. (24)

$$\frac{\varepsilon_0}{\gamma} + \frac{1}{\alpha\gamma}\left\{\left[\frac{\nu-\alpha}{2}\varepsilon_0 + \gamma\right]\exp\left(-\frac{\nu+\alpha}{2}T\right) - \left[\frac{\nu+\alpha}{2}\varepsilon_0 + \gamma\right]\exp\left(-\frac{\nu-\alpha}{2}T\right)\right\} = 0. \quad (26)$$

We can express ε_0 in terms of T with the help of Eq. (25) or (26).

The second relation between ε_0 and T can be obtained from Eq. (14), where $\delta = \zeta(T; \varepsilon_0)$ is determined by formula (10) or (11) depending on the relation between γ and ν. We do not show them here explicitly as they are too lengthy to present. Substituting $\varepsilon_0(T)$ [obtained from Eq. (25) or (26)] into the second relevant relation of ε_0 and T and solving the transcendental equation, one can first calculate T_{SCL}, then $\varepsilon_{0,SCL}$ from Eq. (25) or (26), and finally δ_{SCL} from Eq. (10) or (11).

In Figs. 5(a) and 5(b), dependencies of δ_{SCL} and δ_0 on ν are presented for a set of γ values. Here, δ_{SCL} and δ_0 are the dimensionless diode length for *SCL* and zero-point, respectively. The *SCL* point corresponds to the steady state with maximum current density which obeys the following relation with the inter-electrode gap: $J_{SCL} \sim \delta_{SCL}^2$. Thus, we can infer that the presence of collision reduces the maximum current density at the space charge limit.

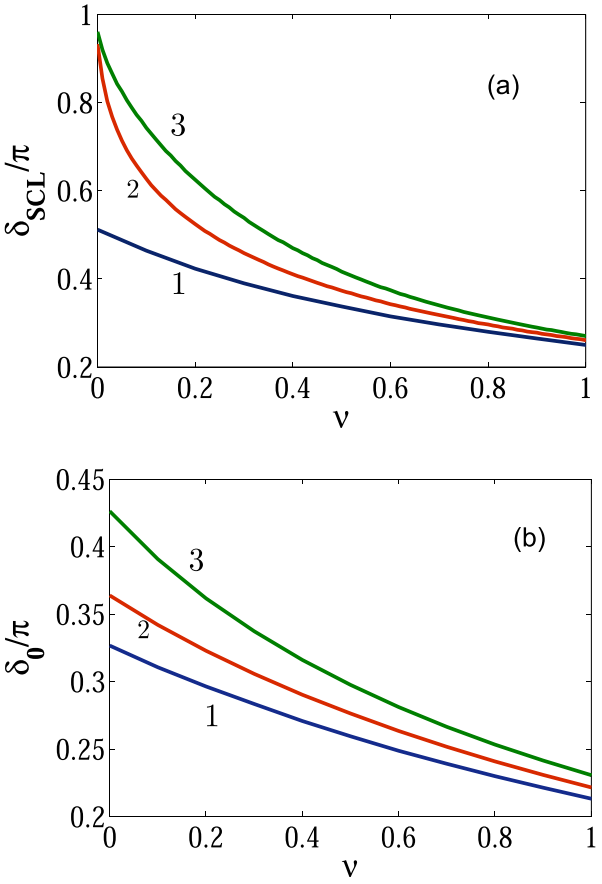

FIG. 5. Dependencies of normalized inter-electrode gap [(a) for *SCL* (δ_{SCL}/π) and (b) for zero-point (δ_0/π)] of the Bursian family on collision frequency (ν) for $\gamma = 0.5$ (curve 1), 1 (2), 1.5 (3). $V = 0$.

IV. CONCLUSION

In this article, we have studied the stationary states of a generalized Pierce diode by the Lagrange technique. The effect of collision has been assimilated through a simplified one-dimensional model. Analytical formulas for the electron trajectories as well as for the potential and the electric field have been obtained. It was found that the potential profile is a wavy-type function for zero and relatively weak collisional effect. This wavy PD brings a new family of solutions which exists along with the Bursian one. With the increasing value of the dimensionless collision frequency, the wavy nature of the potential profile is lost. As a result, the non-Bursian branches disappear and only Bursian branches remain. The steady states are observed for both positive and negative values of the emitter electric field.

We compared our obtained results for the stationary states with the steady states of the non-neutral plasma diode in the presence of the external magnetic field. It is observed that both collision and transverse magnetic field have a similar type of effect on the time-independent states. This similarity is connected by the fact that the beam-like form of the electron velocity distribution function gets deformed in the presence of the external magnetic field or the electron collision.

The effects of cesium pressure on nonlinear oscillations in the Knudsen TIC were experimentally studied (see, Refs. 8 and 9). It was found that the oscillation amplitude starts to quench when the scattering path of electrons and cesium atoms turns out to be comparable with the diode gap. Such oscillations are strongest in the over-neutralized situation when there are more ions than electrons at the emitter, and the steady states of the TIC are characterized by a monotonically increasing potential distribution. It exhibits a quasineutral plasma region with nearly constant potential, embedded between two space-charge sheaths adjacent to the electrodes. The electrons are greatly accelerated by a potential jump near the emitter and enter into the plasma keeping a small velocity spread. In this case, the steady states of a TIC can be successfully modeled by means of the Pierce-like diode in which injected electrons have the beam-like velocity distribution.[18] Therefore, the results obtained in the current paper give grounds to clearly interpret the experimental data obtained from the Knudsen TIC.[8,9]

It would be an interesting problem to investigate the stability properties of the time-independent solutions of a non-neutral plasma as well as the case where some of the electrons are reflected back due to an electron collision. It will be explored next for the future publications. Such studies shall refine our knowledge on diode physics.

ACKNOWLEDGMENTS

One of the authors (Dr. Sourav Pramanik) would like to express his gratitude to the Science and Engineering Research Board (SERB), Department of Science and Technology, India, for providing National Post Doctoral Fellowship for this work (the Fellowship Reference No. PDF/2017/001132).

[1]R. G. McIntyre, J. Appl. Phys. **33**, 2485 (1962).
[2]N. Rynn and N. D'Angelo, Rev. Sci. Instrum. **31**, 1326 (1960).

[3]R. W. Motley, *Q-Machine* (Academic Press, 1975).
[4]E. A. Coutsias and D. J. Sullivan, Phys. Rev. A **27**, 1535 (1983).
[5]W. Hertz, Phys. Technol. **10**, 195 (1979).
[6]V. I. Babanin, I. N. Kolyshkin, V. I. Kuznetsov, V. I. Sitnov, and A. Ya. Ender, "Physics of thermionic energy converters," in *2nd Intersociety Conference on Nuclear Power Engineering in Space*, Sukhumi, Georgia (Vekua Institute of Physics and Technology, Sukhumi, 1991), p. 9.
[7]V. I. Babanin, Yu. A. Dunaev, A. S. Mustafaev, V. I. Sitnov, and A. Y. Ender, Sov. Phys. Tech. Phys. **18**, 1210 (1974).
[8]I. G. Gverdtsiteli, V. Ya. Karakhanov, E. A. Kashirskii, R. Ya. Kucherov, and Z. A. Oganezov, Sov. Phys. Tech. Phys. **17**, 78 (1972).
[9]V. I. Babanin, I. N. Kolyshkin, V. I. Kuznetsov, A. S. Mustafiev, V. I. Sitnov, and A. Y. Ender, Sov. Phys. Tech. Phys. **27**, 793 (1982).
[10]V. I. Kuznetsov and A. Ya. Ender, Sov. Phys. Tech. Phys. **28**, 1431 (1983).
[11]V. R. Bursian and V. I. Pavlov, Zh. Russ. Fiz.-Khim. O-va. **55**, 71 (1923) (in Russian).
[12]J. R. Pierce, J. Appl. Phys. **15**, 721 (1944).
[13]V. I. Babanin, A. Ya. Ender, I. N. Kolyshkin, V. I. Kuznetsov, V. I. Sitnov, and D. V. Paramonov, "Next generation solar bimodal systems," in *Proceedings of the 32rd IECEC* (AIChE, 1997), p. 427.
[14]S. Pramanik, A. Ya. Ender, V. I. Kuznetsov, and N. Chakrabarti, Phys. Plasmas **22**, 042110 (2015).
[15]S. Pramanik, V. I. Kuznetsov, and N. Chakrabarti, Phys. Plasmas **22**, 082103 (2015).
[16]S. Pramanik, V. I. Kuznetsov, A. B. Gerasimenko, and N. Chakrabarti, Phys. Plasmas **23**, 062118 (2016).
[17]V. I. Kuznetsov, S. Pramanik, A. B. Gerasimenko, and N. Chakrabarti, Phys. Plasmas **24**, 023107 (2017).
[18]A. Ya. Ender, S. Kuhn, and V. I. Kuznetsov, Phys. Plasmas **13**, 113506 (2006).
[19]B. B. Godfrey, Phys. Fluids **30**, 1553 (1987).
[20]W. S. Lawson, Phys. Fluids B **1**, 1483 (1989).
[21]S. Kuhn, Phys. Fluids **27**, 1834 (1984).
[22]A. Ya. Ender, H. Kolinsky, V. I. Kuznetsov, and H. Schamel, Phys. Rep. **328**, 1 (2000).
[23]A. Ya. Ender, V. I. Kuznetsov, H. Schamel, and P. V. Akimov, Phys. Plasmas **11**, 3212 (2004).
[24]V. I. Kuznetsov and A. Ya. Ender, Plasma Phys. Rep. **36**, 226 (2010).
[25]V. I. Kuznetsov and A. Ya. Ender, Tech. Phys. **58**, 1705 (2013).
[26]P. V. Akimov and H. Schamel, J. Appl. Phys. **92**, 1690 (2002).
[27]M. V. Nezlin, *Physics of Intense Beams in Plasmas* (IOP, Bristol, 1993).